Electronic Excitation in a Saturated Chain: An MS-CASPT2 Treatment of the Anti Conformer of *n*-Tetrasilane

Raül Crespo* and Manuela Merchán

Departament de Química Física, Universitat de València, Dr. Moliner 50, Burjassot, E-46100 València, Spain

Josef Michl*

Department of Chemistry and Biochemistry, University of Colorado, Boulder, Colorado 80309-0215

Received: May 31, 2000

The singlet−singlet electronic spectrum of the anti conformer of *n*-tetrasilane has been studied using multiconfigurational wave functions (CASSCF), second-order perturbation theory (CASPT2), and its multistate extension (MS-CASPT2), in conjunction with large ANO-type basis sets including Rydberg functions. The calculations include the 4s, 4p, and 3d members of the Rydberg series converging on the first ionization. Mixing of valence and Rydberg states observed in the CASSCF wave functions is not fully rectified by single-reference CASPT2 theory, whereas the MS-CASPT2 method separates the valence and Rydberg states effectively. At the MS-CASPT2 level, six valence excited states have been found below the lowest Rydberg transition, predicted at 7.40 eV. In terms of natural orbitals, they correspond to single electron promotions from the σ-symmetry HOMO to four σ^* and two π^* valence orbitals. Vertical dipole-allowed valence transition energies (oscillator strengths) are computed at 6.33 eV (1.12), 6.68 eV (0.01), and 6.96 eV (0.15), for excitation to 1^1B_u, 1^1A_u, and 2^1B_u states, respectively. Three vertical dipole-forbidden valence transitions are predicted to be interleaved among them at 6.55 eV (2^1A_g), 6.87 eV (3^1A_g), and 7.10 eV (1^1B_g). The results are consistent with the available experimental data and are easily rationalized in terms of a simple Hückel model of σ delocalization.

Introduction

Electronic excitation in saturated organic molecules[1−3] has been attracting increasing interest, at least in part motivated by the anticipated move of nanolithography into the vacuum UV region.[4] Unlike the delocalization and excitation of π electrons, which are quite well understood qualitatively and can be accounted for quantitatively by a variety of semiempirical and more recently also ab initio methods, the delocalization and excitation of σ electrons remain somewhat mysterious. Measurements in the vacuum UV are more difficult, as are the experimental identification of presumably quite densely spaced individual excited states and the separation of the often broad and featureless valence from Rydberg bands. A further complicating feature is the greatly perturbed nature of Rydberg states in condensed phases, in which many of the compounds of interest need to be measured. Computations are plagued by similar problems, in that large numbers of states of similar energy, some diffuse and some not, need to be treated simultaneously.

Saturated compounds of the heavier congeners of carbon, in particular silicon, are easier to examine experimentally than hydrocarbons, since they absorb at notably lower energies. We believe that the shift of their first excited singlet states into the near-UV is related to the lower electronegativity of the heavier elements of group 14 of the periodic table.[5] The obvious relation to the intriguing silicon-based polymers, the polysilanes,[6] provides an additional motivation for their study.

Spectroscopic properties of the parent saturated linear oligosilanes *n*-Si_nH_{2n+2} ($n \geq 2$) have already received considerable experimental and theoretical scrutiny.[1,6−8] Assignments of their broad and featureless UV absorption bands both to valence and Rydberg transitions have been proposed (see discussion in refs 1 and 7). Chain-length and conformational effects on the electronic spectra of the parent and the much more stable fully alkylated oligosilanes and polysilanes provide evidence for strong σ delocalization.[6,9−13] Conformational effects are especially interesting. Interconversion of the conformers involves mainly rotations around single bonds, i.e., a variation of the SiSiSiSi dihedral angles, while other structural changes are only minor. In *n*-Si_nH_{2n+2}, each internal Si−Si bond can be in a gauche or an anti form, in *n*-$Si_n(CH_3)_{2n+2}$ the choices are gauche, ortho, and transoid,[10,14,15] and longer alkyl substituents offer an even wider range of possibilities.[16−18]

The simplest oligosilane for which the relationship between conformational properties and electronic spectra can be studied is *n*-tetrasilane, *n*-Si_4H_{10}, whose gauche and anti forms have similar ground-state energies.[7] An understanding of this species appears indispensable to any efforts to understand the effect of conformations on longer oligosilane chains. The UV spectrum of *n*-Si_4H_{10} in an N_2 matrix at 12 K, which contains both conformers, shows two broad bands with maxima at 6.14 and 6.89 eV.[7] In the classical interpretation,[1,6,19] the intense lowest singlet−singlet transition in oligosilanes is of $\sigma\sigma^*$ character. Its energy is considered to be conformationally dependent and significantly lower in the "well σ-conjugated" anti than in the "poorly σ-conjugated" gauche conformer, accounting for the two peaks in the spectrum of the matrix-isolated anti/gauche mixture of *n*-Si_4H_{10}. However, subsequent experimental evidence suggested a different interpretation of conformational effects on the absorption spectra of tetrasilanes, according to

10.1021/jp001973o CCC: $19.00
Published on Web 08/24/2000

which all conformations have two low-energy B states (in the syn and anti planar limits, one of these is of the $\sigma\sigma^*$ and the other of the $\sigma\pi^*$ type), and it is not so much their energy as their relative intensity that suffers a pronounced change as the SiSiSiSi dihedral angle is varied.[7,9,10] This reinterpretation of the spectra was rationalized in terms of a two-state model, invoking an avoided crossing between B-symmetry $\sigma\sigma^*$ and $\sigma\pi^*$ states along the torsion coordinate. Several previous calculations at the CIS and CASSCF levels[7−10] qualitatively supported this picture and suggested the presence of two weak additional transitions into states of A symmetry in the same spectral region, undergoing a similar avoided crossing. One of these additional transitions was subsequently indeed observed in alkylated tetrasilanes confined to small dihedral angles.[20] A recent CIS study,[8] which also explicitly considered the effects of the matrix environment, concluded that all observed transitions in the near-UV region are into states of valence nature and predicted a series of Rydberg states at higher energies. Nevertheless, so far, the inherent limitations of all previous theoretical studies have prevented a detailed, quantitative, and truly reliable description of the electronic spectrum of *n*-tetrasilane.

As a step toward a better understanding of the spectral behavior of *n*-tetrasilane, we report here a comprehensive theoretical investigation of the nature of the low-lying excited states in the anti conformer at a considerably higher level of ab initio computation than any of the previous attempts. Our aim is to provide a theoretically based interpretation of the absorption spectrum, to reach conclusive assignments for this fundamental species, and to use the resulting experience as a guide for calculations on electronically excited states of other saturated chromophores.

There are a number of open questions. What level of ab initio calculation is needed to obtain quantitative (±0.2 eV error in excitation energies) agreement with the observed contribution of the anti conformer to the lowest singlet−singlet transition? How many valence excited states are located below the lowest Rydberg transition? What are the requirements imposed on the theory by the desire to achieve an accurate identification of the valence and Rydberg states? We shall find that the previous descriptions are largely vindicated, but the situation is shown to be even more complicated than previously suspected, in that a total of six, rather than four, valence excited states are predicted below the Rydberg region. The two new states are at higher energies than the previously known four and their experimental detection presents a challenge.

We have characterized the low-lying valence and Rydberg excited states of the planar anti *n*-Si_4H_{10} conformer by using multiconfigurational second-order perturbation theory as embodied in the CASPT2 method.[21,22] In addition, the indirect interaction of the resulting states has been taken into account within the framework of the recently developed multi-state CASPT2 (MS-CASPT2) method.[23] The successful performance of the CASPT2 approach to the interpretation of the electronic spectra has by now been well established on a large number of unsaturated organic compounds and transition metal complexes.[24,25] So far, however, experience with saturated molecules and silicon-containing compounds is quite limited. A full theoretical description of the spectrum of the anti conformer of *n*-tetrasilane thus is of value both in itself and as an assessment of the ability of current computational methods to handle saturated molecules. As will be seen, the somewhat unusual nature of the excited states of *n*-tetrasilane makes an accurate treatment particularly challenging for ab initio methodology.

Theoretical Methods and Computational Details

The ground-state structure of the anti conformer of *n*-Si_4H_{10} optimized at the MP2(FC)/MC-311G** level and employed in a prior CIS study[8] was used to calculate vertical transition energies and oscillator strengths. The computations were carried out within the C_{2h} symmetry point group constraints, with the silicon atoms placed in the *xy* plane and the *y* axis parallel to the terminal SiSi bonds.

Generally contracted basis sets of the atomic natural orbital (ANO) type were employed and were obtained from Si-(17s12p5d)/H(8s4p) primitive sets.[26] These basis sets were designed to treat correlation and polarization effects optimally. The Si[6s5p2d]/H[2s1p] contraction scheme was used. To characterize the lowest Rydberg states, described mainly by singly excited configurations from the highest occupied molecular orbital (HOMO), the basis set was supplemented with a 1s1p1d set of Rydberg-type functions, contracted from a set of 8s8p8d primitive functions and placed at the charge centroid of the ground state of the positive ion. The Rydberg functions were built following a literature procedure.[27] Based on a large number of calibration calculations that we carried out on *n*-tetrasilane, we can confidently conclude that the basis set is flexible enough for a proper description of both valence and Rydberg low-energy states of the system at a moderate computational cost.

The reference wave function and the molecular orbitals were obtained from average CASSCF calculations, where the averaging procedure included all the A_g, B_u, A_u, or B_g symmetry states of interest. The four 1s core orbitals were kept frozen in the form determined by the Hartree−Fock wave function; the 1s electrons were not correlated at the second-order level. The active spaces used and the type of states computed are summarized in Table 1. In all calculations the number of active electrons was six, corresponding to the three Si−Si bonds of the σ-conjugated system. This is a natural truncation, inspired by the semiempririal "Sandorfy C"[28] and "ladder C"[9,29] models of electronic structure of saturated systems. The next better choice would be to also treat as active the 20 electrons of the ten Si−H bonds (in analogy to the Sandorfy H[28] and ladder H[9,29] models), but we cannot afford to assign all valence electrons in a molecule of this size into the active category and will attempt to treat them with perturbation theory.

The active space comprising the σ and σ^* Si−Si bond orbitals is denoted by (3;3;0;0), where the entries indicate the number of active orbitals belonging to the irreducible representations a_g, b_u, a_u, and b_g, respectively, of the point group C_{2h}. The active space was extended to include the corresponding Rydberg orbitals plus the π^*-symmetry Si−H antibonding orbital combinations as appropriate (Table 1).

To take into account the remaining correlation effects, particularly the correlation with the electrons of the Si−H bonds, the CASSCF wave functions were employed as reference functions in a single-state second-order perturbation CASPT2 treatment.[21,22] The coupling of the CASSCF wave functions via dynamic correlation was dealt with by means of the recently developed extended multistate CASPT2 approach, the MS-CASPT2 method.[23] An effective Hamiltonian matrix is constructed where the diagonal elements correspond to the CASPT2 energies and the off-diagonal elements introduce the coupling to second order in the dynamic correlation energy. In this way, all states of a particular symmetry class can be treated simultaneously with the correlation effects on the reference functions included, and the possibly erroneous valence−Rydberg mixing can be removed. Well-known examples of a strong

TABLE 1: CASSCF Wave Functions Employed To Compute Vertical Electronic Excitations and Ionization Potentials of Anti *n*-Tetrasilane

wave function[a]	N_e[b]	states	N_{conf}[c]	N_{states}[d]
		Basis Set: Si[6s5p2d]/H[2s1p] + 1s1p1d Rydberg Functions		
CASSCF(8;3;0;0)	6	^1A_g (HOMO → 4s, $3d_{x2-y2}$, $3d_{xy}$, $3d_{z^2}$)	4627	7
CASSCF(3;5;0;0)	6	^1B_u (HOMO → $4p_x$, $4p_y$)	570	4
CASSCF(3;3;2;0)	6	^1A_u (HOMO → $4p_z$)	280	2
CASSCF(3;3;0;3)	6	^1B_g (HOMO → $3d_{xz}$, $3d_{yz}$)	614	3
		Basis Set: Si[6s5p2d]/H[2s1p]		
CASSCF(4;3;0;0)	6	^1A_g	254	3
CASSCF(3;3;0;0)	6	^1B_u	83	2
CASSCF(3;3;1;0)	6	^1A_u	105	1
CASSCF(3;3;0;1)	6	^1B_g	105	1
CASSCF(3;3;0;0)	5	$1,2^2A_g$	105	2
CASSCF(3;3;0;0)	5	1^2B_u	105	1

[a] In parentheses, the number of orbitals of symmetries a_g, b_u, a_u, and b_g, respectively, of the point group C_{2h}. Number of frozen orbitals: (2;2;0;0). Number of inactive orbitals: (9;9;4;4). Number of occupied SCF MO's: (13;12;4;4). [b] Number of active electrons. [c] Number of configurations in the CASSCF wave function. [d] Number of states included in the average CASSCF wave function.

TABLE 2: Excitation Energies (*E*) and Oscillator Strengths (*f*) for Anti *n*-Tetrasilane [Si[6s5p2d]/H[2s1p] + 1s1p1d (Rydberg Functions) ANO-Type Basis Set][a]

	CASSCF		CASPT2		MS-CASPT2		
state	*E*/eV[b]	*f*[c]	*E*/eV[b]	*f*[c]	*E*/eV[b]	*f*[c]	$\langle R^2\rangle$[d]
			Valence Excited States				
1^1B_u	8.50 (7.98)	1.098 (1.542)	6.90 (6.40)	0.891 (1.237)	6.33 (6.36)	1.115 (1.175)	144.9
2^1A_g	6.94 (7.15)	0	7.12 (6.69)	0	6.55 (6.68)	0	158.5
1^1A_u	7.58 (7.39)	0.003 (0.003)	6.86 (6.66)	0.003 (0.002)	6.68 (6.66)	0.005 (0.002)	131.5
3^1A_g	6.46 (7.39)	0	6.76 (6.96)	0	6.87 (6.96)	0	163.4
2^1B_u	8.81 (7.84)	0.275 (0.121)	7.50 (6.88)	0.234 (0.107)	6.96 (6.92)	0.154 (0.165)	180.1
1^1B_g	8.06 (7.82)	0	7.51 (7.12)	0	7.10 (7.12)	0	137.7
			Rydberg Excited States				
4^1A_g (HOMO → 4s)	7.10	0	7.33	0	7.40	0	263.1
3^1B_u (HOMO → 4p)	7.76	0.051	7.09	0.046	7.46	0.006	237.2
2^1A_u (HOMO → 4p)	7.60	0.003	7.28	0.003	7.46	0.000	242.4
5^1A_g(HOMO → 3d)	7.29	0	7.87	0	7.86	0	326.1
4^1B_u(HOMO → 4p)	7.79	0.279	7.13	0.255	7.87	0.029	266.5
2^1B_g(HOMO → 3d)	7.78	0	7.74	0	7.93	0	310.3
6^1A_g(HOMO → 3d)	7.61	0	7.70	0	7.99	0	352.6
3^1B_g(HOMO → 3d)	7.84	0	7.84	0	8.10	0	336.8
7^1A_g(HOMO → 3d)	7.76	0	8.09	0	8.22	0	333.8

[a] The character and ordering of the states are those obtained with the MS-CASPT2 method. [b] Excitation energy. Values in parentheses were obtained with the Si[6s5p2d]/H[2s1p] valence basis set. [c] Oscillator strength. [d] Expectation value of R^2 in atomic units. For the ground state, $\langle R^2\rangle = 127.3$.

valence−Rydberg interaction at the CASSCF level are the excited states of ethene and butadiene.[23,30] A similar situation obtains in *n*-tetrasilane and we find that average CASSCF calculations lead to a strong mixing of the Rydberg and valence states. The MS-CASPT2 method is able to rectify the problem, yielding an effective separation of the computed states, which can be clearly identified as either valence or Rydberg.

The CASSCF state interaction (CASSI) method[31,32] was used to calculate the transition dipole moments. In the formula for the oscillator strength, the energy differences obtained in the CASSCF, CASPT2, and MS-CASPT2 computation, respectively, were used as appropriate for each level of calculation. The transition dipole moments computed with the CASSCF wave functions were used in the calculation of both the CASSCF and CASPT2 oscillator strengths. The MS-CASPT2 oscillator strengths were computed using perturbation modified CAS (PMCAS) reference functions (the model states);[23] i.e., linear combinations of all CAS states involved in the MS-CASPT2 calculation.

All calculations were performed with the MOLCAS-4 quantum chemistry software.[33]

Results and Discussion

The vertical excitation energies of the singlet valence and Rydberg excited states of anti *n*-tetrasilane obtained by the CASSCF, CASPT2, and MS-CASPT2 calculations, together with the respective oscillator strengths and transition moment directions, are compiled in Table 2. The last column contains the expectation values of R^2, which clearly differentiate valence and Rydberg states.

In terms of the natural orbitals (NOs) of the PMCAS wave functions obtained with the basis set containing Rydberg functions, the excited states listed in Table 2 can all be characterized as one-electron promotions from the highest occupied molecular orbital (HOMO), $13a_g$ in the closed-shell Hartree−Fock description of the ground state, into different virtual orbitals. For each excited state, the occupation numbers of two NOs are close to unity. One of these NOs is essentially the same for all excited states and also visually indistinguishable from the HOMO obtained from a closed-shell HF calculation (the starting orbital shown in Figure 1 is an NO of the 1^1B_u state). It is bonding across each of the three Si−Si bonds and contains nodes at the two internal Si atoms. The other singly occupied NO is different for each excited state, as shown in Figure 1 for the valence states. For Rydberg excited states, these orbitals have the expected s, p, and d shapes and are not shown.

Valence States. At the highest level of theory employed (MS-CASPT2), six valence excited states occur below the lowest Rydberg transition. These valence excited states are computed to lie within the narrow energy range 6.3−7.1 eV. The first

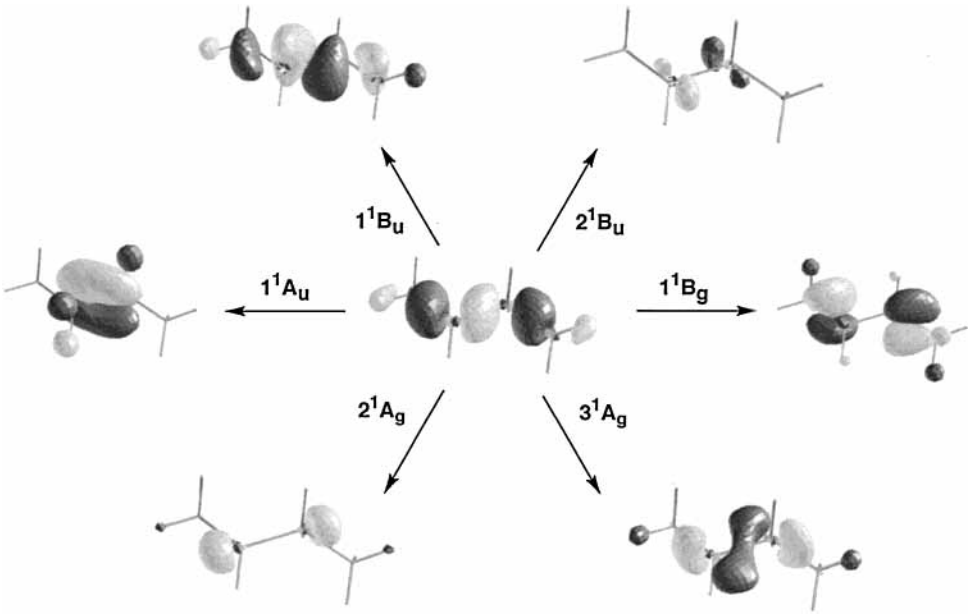

Figure 1. Natural orbitals with occupation numbers close to unity obtained from the Perturbation Modified CAS (PMCAS) wave functions (model states involved in the MS-CASPT2 calculation) of the valence excited states of anti *n*-tetrasilane. The arrows indicate schematically the one-electron promotion nature of the valence excited states from the σ HOMO (center) to the σ^* and π^* valence NOs. The isodensity surface value for the orbitals is 0.043.

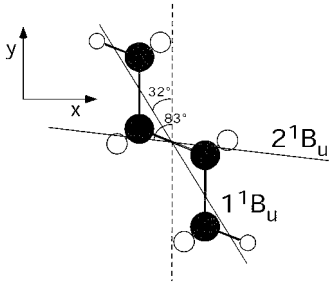

Figure 2. Transition moment directions for the 1^1B_u and 2^1B_u valence states computed at the CASSI level using perturbation modified CAS (PMCAS) wave functions.

four are similar to states calculated previously at lower levels of theory,[7,8] while the highest two (2^1B_u and 3^1A_g) are new.

Strong electronic transitions involve two valence singlet excited states of B_u symmetry and appear at 6.33 and 6.96 eV (Table 2). The expected HOMO−LUMO $\sigma\sigma^*$ 1^1B_u state is associated with the lowest singlet−singlet electronic transition of the molecule, with the largest oscillator strength, around 1.12, and a transition moment directed in the direction of the silicon backbone. It can be clearly attributed to the low-energy experimental band with a maximum at 6.14 eV in the matrix spectrum.[7] The other allowed $\sigma\sigma^*$ electronic transition, from the ground to the 2^1B_u state, has a smaller computed oscillator strength of 0.15 and a transition moment directed along the central Si−Si bond. It probably contributes to the overall shape of the intense high-energy band observed at 6.89 eV in the matrix spectrum.[7] The directions of the two in-plane transition moments are shown in Figure 2. An out-of-plane polarized transition to a very weakly allowed 1^1A_u state is predicted at 6.68 eV, at the red edge of the second observed band, but probably does not affect the observed spectrum noticeably. The bulk of the second observed band is undoubtedly due to the gauche conformer.[7]

In addition, three low-lying dipole-forbidden electronic transitions to the 2^1A_g ($\sigma\sigma^*$), 3^1A_g ($\sigma\sigma^*$), and 1^1B_g ($\sigma\pi^*$) valence excited states are predicted at 6.55, 6.87, and 7.10 eV, respectively. These presumably make entirely negligible contributions to the observed spectrum. The 3^1A_g state lies outside of the active space (3;3;0;0), which involves only the valence σ and σ^* MO's of the Si−Si bonds (there is only one valence Si−Si σ^* orbital of a_g symmetry). Thus, the minimum active space required to describe the valence singlet excited states of A_g symmetry is (4;3;0;0) (six active electrons). Clearly, neither the out-of-plane nor the in-plane Si−H σ orbitals can be neglected in the description of the low-lying valence excited states. The former are needed for the description of the 1^1A_u and 1^1B_g $\sigma\pi^*$ states, the latter are needed for the 3^1A_g $\sigma\sigma^*$ state. The Si−H bonds are an essential part of the *n*-tetrasilane chromophore.

Rydberg States. The calculated vertical transition energy from the ground to the lowest Rydberg state, 4^1A_g (HOMO → 4s), is 7.40 eV. It is placed at 7.10 eV at the CASSCF level, and the effect of dynamic correlation on the excitation energy is only 0.3 eV. At the CIS level, the lowest Rydberg transition energy was computed to be 7.70 eV (the result obtained with basis set IV in ref 8), in reasonable agreement with the present result. However, this state is located below the computed CIS valence excited state of the same symmetry, in disagreement with the more reliable current result. The relatively large differential dynamic correlation effects between the valence and Rydberg states, which are not treated on equal footing at the CIS level, cause the CIS valence state to appear at an energy that is too high, close to that of the ^1A_g (HOMO → 4s) Rydberg state.

At the MS-CASPT2 level, transitions to the 3^1B_u (HOMO → 4p) and 2^1A_u (HOMO → 4p) Rydberg states are found to be essentially degenerate at 7.46 eV, and the latter has an exceedingly weak predicted intensity. Transition to the 4^1B_u (HOMO → 4p) Rydberg state, placed at 7.87 eV, has a predicted oscillator strength of 0.03. The five members of the dipole-forbidden 3d series have been computed to lie in the energy range 7.9−8.2 eV. Therefore, in agreement with the conclusion reached in a CIS study,[8] Rydberg-type transitions have no detectable influence on the reported matrix absorption spectrum of tetrasilane,[7] and the same would be true even in the gas phase.

The present results confirm the long tradition of interpreting the observed features as predominantly valence in character.[1,7]

Ionized States. At the CASPT2 (CASSCF) level, the first, second, and third vertical ionization potentials of anti *n*-tetrasilane are computed to be at 9.32 (9.19), 10.48 (10.68), and 10.64 (10.70) eV and are related to the 1^2A_g, 2^2A_g, and 1^2B_u states of the radical cation, respectively. Thus, the first and second ionization potentials are separated by about 1.2 eV. As a result, the corresponding members of the Rydberg series converging to these two ionization potentials are expected to lie about 1.2 eV apart. As the energies of the computed Rydberg electronic transitions differ by 0.82 eV, the early members of the Rydberg series leading to the two ionization potentials are not expected to overlap. The reported photoelectron spectrum of an anti-gauche conformer mixture contains severely overlapping peaks at 9.62, 10.3, and 10.85 eV, and after approximate deconvolution, the original authors suggested the value of 9.36 eV as the best guess for the first ionization potential of the anti conformer.[34] The agreement between theory and the published interpretation of the experiment is excellent.

The Absence of Valence−Rydberg Mixing. The difference between the CASSCF and MS-CASPT2 excitation energies can be considered as a measure of the contribution of dynamic correlation to the energy of a state. A comparison between the CASSCF and MS-CASPT2 results demonstrates that dynamic correlation effects contribute the most to lowering the excitation energy of the lowest valence excited state 1^1B_u (over 2 eV). Even the CASPT2 method places this state too high by 0.57 eV. High dynamic correlation is typically found in zwitterionic states, i.e., those with a large weight of hole-pair structures in the valence bond (VB) description. The present result thus is in full accord with the characterization of the 1^1B_u state as zwitterionic, described by VB structures such as H_3Si^+ H_2Si^-−SiH_2−SiH_3, and the dynamic correlation is with electrons in the Si−H bonds. That is expected from a simple-minded description of σ-delocalized and π-delocalized systems as analogous, cf. the zwitterionic states of ethene and butadiene.[30] It is therefore not surprising that the CIS method also produces a large deviation; the CIS result for the 1^1B_u state is 7.14 eV.[8]

In summary, in anti *n*-Si_4H_{10}, a four-roots average CASSCF calculation of ^1B_u symmetry states leads to a spurious valence−Rydberg mixing that a single-reference multiconfigurational second-order perturbation theory such as CASPT2 does not fully rectify, yielding two valence states 1^1B_u and 2^1B_u placed too high and two Rydberg states located too low in energy. Transition to the 4^1B_u (HOMO → 4p) Rydberg state is computed to have significant oscillator strength at the CASSCF and CASPT2 levels, which reflects the incorrectly admixed valence contribution to this Rydberg state. The MS-CASPT2 method leads to an effective separation of the four excited states into two valence and two Rydberg states.

It should be noted that similar results for the valence excited states are obtained at the MS-CASPT2 level with both basis sets, with and without Rydberg functions. Furthermore, when the valence basis set is employed (results within parentheses in Table 2) the CASPT2 and MS-CASPT2 results agree. Thus, once the number of valence states is known, a proper description of the valence excited states can already be achieved at the CASPT2 level, using the Si[6s5p2d]/H[2s1p] valence basis set. However, prior knowledge of the correct number of valence states is important, otherwise valence−Rydberg mixing still occurs despite the valence character of the basis set. For instance, when three roots of ^1B_u symmetry are computed with the Si-[6s5p2d]/H[2s1p] valence basis set, the nice agreement of the results with respect to the findings obtained with the extended basis set is destroyed, since the CASSCF calculation tries to make the extra root as diffuse as the basis set allows. The actual number of valence excited states present in a given energy region can only be determined when a full computation including both valence and Rydberg states is undertaken. Of course, a flexible enough basis set has then to be supplied and the interaction of the states taken into account in order to overcome the possibly erroneous valence−Rydberg mixing. The MS-CASPT2 method, in conjunction with a Rydberg basis set constructed as mentioned above, appears to represent a reliable approach for this purpose. The valence−Rydberg mixing also occurs at the CIS level. As a result, the second valence state of ^1B_u symmetry is missing at that level of approximation.[8]

Relation to the Ladder H Model. The fact that each of the six valence excitations can be described by a single electron promotion from the HOMO to an orbital of a σ^* or π^* character, using NOs extracted from the complicated PMCAS wave functions, suggests that it might be possible to mimic the ab initio results with a simple properly parametrized empirical scheme, which could then be useful for all conformations of much larger oligosilanes, and perhaps even for the polysilane high polymers.

To be useful, such a scheme would have to be able to handle all of the valence states even if just the lowest or the most intense one or two transitions are of interest. Even though in the anti conformer of *n*-tetrasilane only transitions into ^1B_u states are intense and transitions to the ^1A_g and ^1B_g states are forbidden altogether, other conformations are not centrosymmetric, only the A and B symmetry classes exist, and all transitions are allowed. In longer oligosilanes, symmetry will freqently be even lower. As the molecular conformation is changed, avoided crossings occur between states that carry absorption intensity and those that do not,[7−10] and it would be foolhardy to dismiss some of these states as unimportant in an a priori fashion. We concluded above that in-plane as well as out-of-plane Si−H antibond orbitals are essential for the description of valence excited states. Therefore, in any future attempts to model the excited states of oligosilanes, and probably other saturated molecules as well, the more complex H-type models,[9,28,29] whose basis sets include substituent orbitals, are preferable to the simpler C-type models,[9,28,29] which are restricted to backbone orbitals. Since the Sandorfy H model[28] does not contain any dependence of interaction integrals on dihedral angles, it is clearly unsuitable for the modeling of the conformational dependence of absorption spectra, and we are left with the ladder H approximation[9,29] as the only possibly adequate candidate for a simple model of the excited states of saturated molecules.

In this regard, the form of the NOs shown in Figure 1 is highly encouraging, in that they have almost exactly the expected appearance. In the simplest qualitative ladder H description of an anti *n*-tetrasilane at the Hückel level,[6−10] the eight Si sp^3 hybrid orbitals and the two substantially more electronegative hydrogen 1s orbitals located in the plane of the molecule are combined to form two Si−H σ and two Si−H σ^* localized bond orbitals and three σ plus three σ^* delocalized Si−Si MO's of the backbone. The four antisymmetric combinations of the lateral antibonding Si sp^3 hybrid−H 1s antibond pairs are used to form four antibonding π^* MO's. The remaining orbitals are not needed for the construction of the valence excited configurations required.

In this simple scheme, the delocalized backbone Si−Si σ and σ^* MO's alternate betwen a_g and b_u symmetry as their energy increases. The HOMO (a_g), in which all the excitations originate,

is bonding across all three SiSi bonds and has two nodes, one at each of the internal Si atoms (not counting the internal nodes at each Si atom), cf. Figure 1. The terminating σ^* orbital for the 1^1B_u state is the LUMO (b_u). It has three nodes, one across each SiSi bond. The next higher σ^* orbital, a_g, is the terminating orbital for the 2^1A_g state and has four nodes (Figure 1; in the schematic representation in Figure 3 of ref 8, the central SiSi bond in this orbital is not drawn well). The third σ^* orbital, b_u, is the terminating orbital for the 2^1B_u state and should have five nodes in the simple picture. In this case, the similarity is imperfect and the NO of Figure 1 only meets the simple expectations (a node across each of the three SiSi bonds and a node at each internal Si atom) in the region of the central SiSi bond. Its diffuse density outside of the bond regions suggests that it has partial Rydberg character, as is also clear from its larger $\langle R^2 \rangle$ value (Table 2). This could well be an artifact due to an incomplete suppression of the mixing of valence and Rydberg states for this highest valence state, even at the MS-CASPT2 level of calculation.

Finally, there is an additional σ^* orbital of a_g symmetry that is the terminating NO for the 3^1A_g state and is bonding across the central SiSi bond. This orbital is absent in the above description, which contains only the three Si−Si σ^* orbitals, and its considerable amplitude on the in-plane hydrogen atoms attached to the terminal silicons suggests that the in-plane Si−H σ^* are not really perfectly localized as assumed above for simplicity, but participate in backbone conjugation.

Only two of the four antibonding π^* MO's of the ladder H model are needed. The terminating NO of the 1^1A_u state, a_u, has no nodes across SiSi bonds and corresponds to the most stable of these π^* MO's. The terminating NO of the 1^1B_g state, b_g, is next and has a node across the central SiSi bond. Both NOs look exactly as expected. It remains to be seen whether it is possible to parametrize the ladder H model in a way that would reproduce the ab initio results for a series of oligosilanes at various conformations or whether it will only be useful for qualitative rationalizations of the type presented here. Parametrization against experimental data will be difficult, since even for the best known and simplest case, peralkylated *n*-tetrasilanes, only three of the now expected six valence excited states have been observed so far.[20]

Most of the NOs correspond reasonably well to virtual canonical HF orbitals, and only the terminating orbital of the 2^1B_u state cannot be easily identified with a canonical virtual orbital in the Hartree−Fock description (Figure 1).

Summary and Conclusions

The strong valence−Rydberg mixing that is observed for vertical singlet excited states of the anti conformer of *n*-tetrasilane at lower levels of theory disappears almost entirely when the different electronic states are allowed to couple through second-order energy (MS-CASPT2). Six valence excited states are then found in the energy interval 6.33−7.10 eV, below the lowest Rydberg transition. Each can be characterized by one singly excited configuration involving electron promotion from the σ-symmetry HOMO (a_g) into a valence σ^* orbital. Four promotions are into σ^* and two into π^* orbitals. The $\sigma\sigma^*$ transitions into 1^1B_u (6.33 eV) and 2^1B_u (6.96 eV) states are strongly allowed, those into 2^1A_g and the previously unanticipated 3^1A_g states are dipole forbidden. One of the two predicted transitions into $\sigma\pi^*$ states (1^1A_u) is allowed and the other (1^1B_g) forbidden, and their contribution to the observed absorption intensity is predicted to be negligible. The 4s, 4p, and 3d members of the Rydberg series converging on the first ionization potential, calculated at 9.32 eV, are computed to lie within the energy interval 7.40−8.22 eV.

These results identify all bands observed up to now as valence in character, and the previously also contemplated predominantly Rydberg assignments can be definitely ruled out. We believe that both ^1B_u states are important for the understanding of the contribution of the anti conformer to the absorption spectrum observed in the matrix. The 1^1B_u state is responsible for the low-energy band, and the newly identified 2^1B_u state contributes to the overall shape of the high-energy band, most of which is, however, due to the gauche conformer.

Due to the larger Si^+ Si^- zwitterionic character of the HOMO−LUMO 1^1B_u state, effects of dynamic correlation with electrons of Si−H bonds have a pronounced effect on its computed energy. When dynamic correlation is not taken into account, the two B_u states are nearly degenerate and too high in energy. Whether the HOMO−LUMO ^1B_u state becomes the lowest in a CASSCF wave function or not depends on the details of the calculation (basis set, geometry, etc.). This explains the difficulties encountered previously,[7,8] since dynamical correlation effects were neglected.

The four lowest computed valence states correspond closely to qualitative expectations deduced from a simple Hückel version of the ladder H model, based on one-electron promotions from a delocalized σ HOMO to delocalized valence Si−Si σ^* and Si−H π^* orbitals. The lowest transition into the 1^1B_u state corresponds to HOMO−LUMO excitation, in which one node is added, accounting for its high intensity. The promotion into the next higher σ^* orbital, which adds two nodes and generates the 2^1A_g state, is symmetry forbidden. Promotions into the lowest two π^* orbitals yield the expected weakly allowed out-of plane polarized 1^1A_u state and, at higher energy, the symmetry forbidden 1^1B_g state.

The two newly described states can also be easily described in the above model. The 2^1B_u state corresponds to excitation from the HOMO into the highest valence Si−Si σ^* orbital that can be constructed from Si−Si antibonds alone, adding three nodes, but the correspondence of the actual shape of the computed NO to the shape anticipated from the simple model is imperfect, probably because of some Rydberg character, which may be real or artifactual. The other new state, 3^1A_g, corresponds to a promotion from the HOMO to a valence σ^* orbital that involves the in-plane Si−H σ^* antibonds in addition to Si−Si σ^* antibonds.

It thus appears conceivable that the excitation energies and nature of the wave functions might be reproduced by a simple parametrized semiempirical scheme. If the results carry over to peralkylated oligosilanes, such a scheme would be very useful for prediction and interpretation of the several lowest excitation energies of longer oligosilanes, and perhaps polysilanes as well. In a more general sense, the results raise the hope that low-lying excited states of other saturated molecules might ultimately be amenable to a simple analysis.

Acknowledgment. This work has been supported by the DGES Projects PB97-1381 and PB97-1377, the CICYT Project MAT97-1044 of Spain, and the USARO (DAAG55-98-1-0310).

References and Notes

(1) Robin, M. B. *Excited States of Polyatomic Molecules*; Academic Press: New York, 1974; Vol. 1.

(2) Robin, M. B. *Excited States of Polyatomic Molecules*; Academic Press: New York, 1974; Vol. 2.

(3) Robin, M. B. *Excited States of Polyatomic Molecules*; Academic Press: New York, 1974; Vol. 3.

(4) E.g.: Rothschild, M.; Bloomstein, T. M.; Curtin, J. E.; Downs, D. K.; Fedynyshyn, T. H.; Hardy, D. E.; Kunz, R. H.; Liberman, V.; Sedlacek, J. H. C.; Uttaro, R. S.; Bates, A. K.; Van Peski, V. *J. Vac. Sci. Technol. B* **1999**, *17*, 3262.

(5) Michl, J. *Acc. Chem. Res.* **1990**, *23*, 127.

(6) Miller, R. D.; Michl, J. *Chem. Rev.* **1989**, *89*, 1359.

(7) Albinsson, B.; Teramae, H.; Plitt, H. S.; Goss, L. M.; Schmidbaur, H.; Michl, J. *J. Phys. Chem.* **1996**, *100*, 8681.

(8) Crespo, R.; Teramae, H.; Antic, D.; Michl, J. *Chem. Phys*. **1999**, *244*, 203.

(9) Teramae, H.; Michl, J. *Mol. Cryst. Liq. Cryst.* **1994**, *256*, 149.

(10) Albinsson, B.; Teramae, H.; Downing, J. W.; Michl, J. *Chem. Eur. J.* **1996**, *2*, 529.

(11) Mazières, S.; Raymond, M. K.; Raabe, G.; Prodi, A.; Michl, J. *J. Am. Chem. Soc.* **1997**, *119*, 6682.

(12) Yatabe, T.; Okumoto, H.; Kaito, A.; Ueno, K.; Shen, J.; Ito, K. *Macromolecules* **1998**, *31*, 7483.

(13) Raymond, M. K.; Michl, J. *Int. J. Quantum Chem.* **1999**, *72*, 361.

(14) Albinsson, B.; Antic, D.; Neumann, F.; Michl, J. *J. Phys. Chem. A* **1999**, *103*, 2184.

(15) Ottosson, C. H.; Michl, J. *J. Phys. Chem. A* **2000,** *15*, 3367.

(16) Michl, J.; West, R. In *Silicon-Containing Polymers: The Science and Technology of their Synthesis and Applications*; Jones, R. G., Ando, W., Chojnowski, J., Eds.; Kluwer Academic Publishers: Dordrecht, the Netherlands, in press.

(17) Fogarty, H. A.; Ottosson, C. H.; Michl, J. *J. Mol. Struct*. (THEOCHEM), in press.

(18) Fogarty, H. A.; Ottosson, C. H.; Michl, J. *J. Mol. Struct*., in press.

(19) Balaji, V.; Michl, J. *Polyhedron* **1991**, *10*, 1265.

(20) Imhof, R.; Teramae, H.; Michl, J. *Chem. Phys. Lett.* **1997**, *270*, 500.

(21) Andersson, K.; Malmqvist, P.-Å.; Roos, B. O.; Sadlej, A. J.; Wolinski, K. *J. Phys. Chem*. **1990**, *94*, 5483.

(22) Andersson, K.; Malmqvist, P.-Å.; Roos, B. O. *J. Chem. Phys.* **1992,** *96*, 1218.

(23) Finley, J.; Malmqvist, P.-Å.; Roos, B. O.; Serrano-Andrés, L. *Chem. Phys. Lett.* **1998**, *288*, 299.

(24) Roos, B. O.; Andersson, K.; Fülscher, M. P.; Malmqvist, P.-Å.; Serrano-Andrés, L.; Pierloot, K.; Merchán, M. *Multiconfigurational Perturbation Theory: Applications in Electronic Spectroscopy*; Prigogine, I., Rice, S. A., Eds.; John Wiley & Sons: New York, 1996; p 219.

(25) Merchán, M.; Serrano-Andrés, L.; Fülscher, M. P.; Roos, B. O. *Multiconfigurational Perturbation Theory Applied to Excited States of Organic Compounds*; Hirao, E., Ed.; World Scientific Publishing Company: Amsterdam, 1999; Vol. 4, p 161.

(26) Widmark, P.-O.; Persson, B. J.; Roos, B. O. *Theor. Chim. Acta* **1991**, *79*, 419.

(27) Roos, B. O.; Fülscher, M. P.; Malmqvist, P.-Å.; Merchán, M.; Serrano-Andrés, L. *Theoretical Studies of Electronic Spectra of Organic Molecules*; Langhoff, S. R., Ed.; Kluwer Academic Publishers: Dordrecht, The Netherlands, 1995; p 357.

(28) Sandorfy, C. *Can. J. Chem.* **1955**, *33*, 1337.

(29) Plitt, H. S.; Michl, J. *Chem. Phys. Lett.* **1992**, *198*, 400. Plitt, H. S.; Downing, J. W.; Raymond, M. K.; Balaji, V.; Michl, J. *J. Chem. Soc., Faraday Trans.* **1994**, *90*, 1653.

(30) Serrano-Andrés, L.; Merchán, M.; Nebot-Gil, I.; Lindh, R.; Roos, B. O. *J. Chem. Phys*. **1993**, *98*, 3151.

(31) Malmqvist, P.-Å. *Int. J. Quantum Chem.* **1986**, *30*, 479.

(32) Malmqvist, P.-Å.; Roos, B. O. *Chem. Phys. Lett*. **1989**, *155*, 189.

(33) Andersson, K.; Blomberg, M. R. A.; Fülscher, M. P.; Karlström, G.; Lindh, R.; Malmqvist, P.-Å.; Neogrády, P.; Olsen, J.; Roos, B. O.; Sadlej, A. J.; Schütz, M.; Seijo, L.; Serrano-Andrés, L.; Siegbahn, P. E. M.; Widmark, P.-O. *MOLCAS, version 4.0*; Department of Theoretical Chemistry, Chemical Centre: University of Lund, P.O.B. 124, S-221 00 Lund, Sweden, 1997.

(34) Bock, H.; Ensslin, W.; Fehér, F.; Freund, R. *J. Am. Chem. Soc.* **1976**, *98*, 668.